NeuroImage 122 (2015) 96–104

Contents lists available at ScienceDirect

NeuroImage

journal homepage: www.elsevier.com/locate/ynimg

Default mode network connectivity during task execution

D. Vatansever [a,b,*], D.K. Menon [a,b], A.E. Manktelow [a,b], B.J. Sahakian [c], E.A. Stamatakis [a,b]

[a] Division of Anaesthesia and Department of Clinical Neurosciences, School of Clinical Medicine, University of Cambridge, Cambridge, UK
[b] Wolfson Brain Imaging Centre, University of Cambridge, Cambridge, UK
[c] Department of Psychiatry, School of Clinical Medicine, University of Cambridge, Cambridge, UK

ARTICLE INFO

Article history:
Received 30 January 2015
Accepted 20 July 2015
Available online 26 July 2015

Keywords:
Default mode network
Finger opposition task
Functional connectivity
Graph theory
Hierarchical clustering

ABSTRACT

Initially described as task-induced deactivations during goal-directed paradigms of high attentional load, the unresolved functionality of default mode regions has long been assumed to interfere with task performance. However, recent evidence suggests a potential default mode network involvement in fulfilling cognitive demands. We tested this hypothesis in a finger opposition paradigm with task and fixation periods which we compared with an independent resting state scan using functional magnetic resonance imaging and a comprehensive analysis pipeline including activation, functional connectivity, behavioural and graph theoretical assessments. The results indicate task specific changes in the default mode network topography. Behaviourally, we show that increased connectivity of the posterior cingulate cortex with the left superior frontal gyrus predicts faster reaction times. Moreover, interactive and dynamic reconfiguration of the default mode network regions' functional connections illustrates their involvement with the task at hand with higher-level global parallel processing power, yet preserved small-world architecture in comparison with rest. These findings demonstrate that the default mode network does not disengage during this paradigm, but instead may be involved in task relevant processing.

Introduction

Extensive neuroimaging research has identified a set of brain regions that displays relative deactivation during goal-driven, attention demanding paradigms (Binder et al., 1999; Mazoyer et al., 2001; Shulman et al., 1997). Despite the difficulty in assigning functional significance to these observations, the detected activity in the posterior cingulate, medial prefrontal cortices and bilateral angular gyri has been attributed to a "default mode of brain function" (Raichle et al., 2001), prominent in the absence of any external task demands (Gusnard and Raichle, 2001; Gusnard et al., 2001).

Initial findings reported on the activity/inactivity of default mode regions during cognitive paradigms were later complemented by functional connectivity analyses of task-free functional magnetic resonance imaging (fMRI) data. Acquired during no-task conditions, resting state fMRI has provided remarkable insight into the human brain organization by revealing synchronous oscillations of distant brain regions that form distinct large-scale brain networks (Biswal et al., 1995). Using this technique, Greicius and colleagues advanced our understanding of the default mode brain by showing not only that the same set of regions, which deactivate during cognitive tasks, form an intrinsic default mode network (DMN) at rest (Greicius et al., 2003), but also that this network is mirrored by direct structural connections (Greicius et al., 2009). Further exploration of both rest and task-based fMRI data revealed interactions between DMN and other large-scale brain networks. A prevailing anti-correlation was reported between DMN and dorsal attention networks (Fox et al., 2005) at rest, and DMN coupling with the fronto-parietal control network has been observed during task execution (Spreng et al., 2010). Moreover, the quantification of such neural communication through network level graph theoretical analyses also provided robust support for the economical organization of the brain into biologically relevant complex architecture (Achard et al., 2006; Buckner et al., 2009; Bullmore and Sporns, 2012; Fransson and Marrelec, 2008; Hagmann et al., 2008) with a central role attributed to the DMN (van den Heuvel and Sporns, 2011).

The volume of research demonstrating the existence of the DMN mechanistically is now substantial; nonetheless, explanations for its exact contribution to brain function remain scarce. A meta-analytic comparison of DMN to task-based activation maps (Smith et al., 2009) reported substantial overlap with tasks that encompassed theory of mind, social cognition, episodic recall and imagined scenes (Laird et al., 2011). Furthermore, many task-free studies have all revealed alterations in this network's properties in different patient populations such as Alzheimer's disease (Buckner et al., 2009) and traumatic brain injury (Sharp et al., 2011), following pharmacological interventions

* Corresponding author at: Department of Clinical Neurosciences, Division of Anaesthesia, University of Cambridge, Box 93, Addenbrooke's Hospital, Hills Road, Cambridge CB2 0QQ, UK.
E-mail address: ddsv2@cam.ac.uk (D. Vatansever).
URL: http://www.neuroscience.cam.ac.uk/directory/profile.phpddsv2 (D. Vatansever).

http://dx.doi.org/10.1016/j.neuroimage.2015.07.053

such as propofol (Stamatakis et al., 2010), and with normal ageing (Damoiseaux et al., 2008). Overall, existing evidence advocates for a fundamental, possibly adaptive role that spans a variety of cognitive domains (Hasson et al., 2009; Schacter et al., 2012).

Although not extensively investigated, some recent studies concur with this view by revealing changes in DMN topography during task conditions and alluding to a possible involvement in cognitive processing. Specifically, differential changes in DMN functional connectivity and network properties have been demonstrated in tasks such as working memory, auditory oddball, and autobiographical planning (Arbabshirani et al., 2013; Fransson and Marrelec, 2008; Harrison et al., 2008; Newton et al., 2011; Spreng et al., 2013). Furthermore, there have been claims for a positive relationship between DMN connectivity and performance during a working memory task (Hampson et al., 2006). These studies, which may appear disparate at first sight, display one important commonality: the persistence of DMN functional connectivity during task execution, with some connectivity attenuation during paradigms of high mental load (Fransson, 2006). Given this evidence for DMN reconfiguration and its interaction with other large-scale brain networks during tasks, we would expect DMN to persist and exchange information with task related networks in a variety of experimental paradigms with a comprehensive role that implies direct contribution to cognitive processing.

We discuss here our initial approach to testing this hypothesis during a task of relatively low cognitive demand, in which participants followed visual cues to execute purposeful movement (finger opposition). Our specific questions pertained to the possible task-induced alterations in the DMN topography with potential behavioural significance, and interaction with the task related somatomotor network (SMN). We aimed to identify mechanisms of DMN engagement or disengagement during task and fixation conditions as well as rest by investigating them with activation, functional connectivity, behavioural correlation and graph theoretical analyses. In comparison with traditional subtractive activation/deactivation approaches, such multifaceted analysis could further quantify DMN engagement during task execution. In line with these objectives, our findings provide evidence on the nature and extent of DMN involvement in task execution and may advance our understanding of its contribution to brain function.

Materials and methods

Participants

The study was approved by the local ethics committee and all participants gave informed consent following the presentation of a study specific information sheet. The exclusion criteria comprised of a score below 70 on the National Adult Reading Test (NART) and 23 on the Mini Mental State Exam (MMSE), any history of drug or alcohol abuse, psychiatric and neurological disorders, head injury, medication use affecting cognitive performance (e.g. tricyclic antidepressants), physical handicap hindering the completion of the study, left-handedness, contraindication to MRI scanning and severe claustrophobia. Complying with these conditions, 22 healthy participants were recruited (19–57 years old, mean = 35.0, SD = 11.2, 9/13 female to male ratio) with average scores of 117.1 (SD = 5.76) on NART and 29.33 (SD = 0.85) on MMSE.

Behavioural assessment

The participants were assessed with an extensive set of neuropsychological tests using the Cambridge Neuropsychological Test Automated Battery (CANTABeclipse). In the simple reaction time test the participants were instructed to press a button in response to the visual presentation of a white box stimulus over a black background. Our measure of choice, the mean simple reaction time denoted the speed of motor response, in which shorter latency implied faster processing.

Paradigm specifications

In addition to the 5 min resting state scanning (eyes closed), a self-paced, right-handed finger opposition paradigm was employed in a boxcar design with 5 alternating cycles of task and fixation blocks. A visual "move" command indicated for participants to initiate and repeat the movement, while "rest" signalled the fixation state. The participants were instructed to touch the remaining fingers with their right thumb moving sequentially from the index to little finger, and to continue the cycle for the duration of the task period. Since we did not have access to the scanner compatible equipment to assess speed of finger opposition during task performance, we instead related latencies obtained from the CANTAB simple reaction time task to functional connectivity strengths.

Image acquisition and preprocessing

The MRI data was obtained using a Siemens Trio 3 T scanner at the Wolfson Brain Imaging Centre, Cambridge. The imaging session started with a high resolution T1-weighted, magnetization-prepared 180 degrees radio-frequency pulses and rapid gradient-echo (MPRAGE) structural scan (TR = 2300 ms; TE = 2.98 ms; TA = 9.14 min; flip angle = 9°; field of view (FOV) read = 256 mm; voxel size = 1.0 × 1.0 × 1.0 mm, slices per slab = 176), followed by whole-brain echo planar imaging (EPI) for the resting state scanning and the finger opposition paradigm (TR = 2000 ms; TE = 30 ms; flip angle = 78°; FOV read = 192 mm; voxel size = 3.0 × 3.0 × 3.0 mm; volumes = 160; slices per volume = 32). The preprocessing and image analysis were all performed using the Statistical Parametric Mapping (SPM) Version 8.0 (http://www.fil.ion.ucl.ac.uk/spm/) and MATLAB Version 12a platforms (http://www.mathworks.co.uk/products/matlab/). All imaging data were preprocessed following a standard pipeline of slice-time and motion correction, normalization to the Montreal Neurological Institute (MNI) space in combination with the segmented high-resolution grey matter structural image and an a priori grey matter template, and smoothing with an 8 mm FWHM Gaussian kernel.

Task-induced activation analysis

This analysis was carried out in order to validate the task and to derive a set of regions of interest (ROIs) to be used for subsequent functional connectivity analyses. For each subject, the functional images acquired during the task were entered into a first level general linear model with the fixation and task onsets modelled as regressors convolved with a canonical HRF. Further, the data was temporally filtered with a high pass filter (cut-off of 128 s) and no global normalization was performed. A one-sample t-test examined group level effects for the contrast of *task* > *fixation*. The resulting statistical maps were conservatively corrected for multiple comparisons at the voxel level using family wise error (FWE), alpha = 0.05, and the local peaks were assessed for further use as ROIs in the functional connectivity analyses.

ROI definitions

Depending on their source of identification (anatomical atlas, task or resting state scanning), the definitions of ROIs can have substantial influence on the subsequent functional connectivity and graph theoretical analyses (Smith et al., 2011). Task-based definition is a method shown to reproduce valid network topologies (Dosenbach et al., 2007; Power et al., 2011; Spreng et al., 2013). The employed finger opposition task provided us with 14 somatomotor ROIs, selected according to the local peaks in the *task* > *fixation* contrast of the activation analysis (voxel level multiple comparison correction, FWE $p < 0.05$). Sixteen seeds defining the DMN were chosen from the current literature (Andrews-Hanna et al., 2010). The MNI coordinates and the corresponding

nomenclature for the complete set of 30 ROIs are listed in Table 1. All ROIs were defined as spheres of 6 mm in diameter.

ROI-to-voxel functional connectivity and behavioural correlation analyses

In contrast to traditional activation/deactivation studies, which remove a considerable amount of information relevant to the default mode processing, functional connectivity analysis provides an integrated view of brain function, identifying networks of regions that are hypothesized to work in collaboration both at rest and during task execution. Following this rationale, we focused on the functional connectivity of default mode and somatomotor networks, aiming to investigate the potential changes in their topography under varying experimental conditions.

The assessment of functional connectivity for both the resting state and the finger opposition paradigm scans were carried out using the *Conn* functional connectivity toolbox (Whitfield-Gabrieli and Nieto-Castanon, 2012). A strict noise reduction method called CompCor removed the principal components attributed to white matter and cerebrospinal fluid signals (Behzadi et al., 2007) and eliminated the need for a global signal regression (Chai et al., 2012; Murphy et al., 2009). In addition to the subject-specific six realignment parameters and their first order derivatives, the main effect of scanning condition was also introduced as a potential confound (Fair et al., 2007). Moreover, a temporal filter of 0.009 and 0.08 Hz was applied to focus on low-frequency fluctuations (Fox et al., 2005).

Following these temporal preprocessing steps, an ROI-to-voxel seed-based functional connectivity analysis was performed. For each experimental condition (task, fixation and rest), average BOLD time-series from 6 mm spherical ROIs on the main hubs of the two networks (posterior cingulate cortex for DMN and left precentral gyrus for SMN) were entered into a seed-based functional connectivity analysis for each subject. The correlation maps were then carried forward to second level paired t-tests and one-way ANOVA analyses. Moreover, in order to assess any possible behavioural correlate of the seed connectivity, the DMN maps were also used in a correlational analysis with the mean simple reaction time score from CANTAB as a covariate. All the reported results are cluster corrected at the FWE 0.05 significance level.

ROI-to-ROI correlation and hierarchical clustering analyses

Owing to the observed task-induced deactivations during attention-demanding paradigms, the default mode regions were historically labelled as “task negative”, in contrast to “task positive” regions, which were the areas that responded to the given tasks. This dichotomy has led to the assumption that the default mode regions do not interact with core task related networks. Against this view, we investigated the potential interactions between the default mode and task related somatomotor regions, aiming to reveal possible alterations in their interaction under varying environmental demands. Thus, 30 × 30 matrices of Fisher z-transformed bivariate correlation coefficients (Pearson r) were constructed using all of the 30 ROIs identified from the activation analysis and selected from the literature. These weighted correlation matrices formed the basis of the connectomic representations for ROI-to-ROI functional connectivity. A hierarchical clustering analysis that positioned functionally similar areas in one of the two domains (default mode and somatomotor) was conducted to identify any ROIs that changed their network membership. Higher numbers of clusters (4, 6 and 8) were also employed to assess the effect of cluster definition on the network alignments (unpublished data). The overall default mode and somatomotor system partition did not change with the increasing number of clusters. The results were FWE corrected ($p < 0.05$) at the seed and network levels using Network Based Statistics (NBS)—a method that relies on non-parametric permutation testing of network intensity (Zalesky et al., 2010).

Graph theoretical analysis

Following a qualitative assessment of the default mode and somatomotor regions' ROI-to-ROI interactions under rest and task conditions, our next aim was to quantify the potential changes in network architecture. Graph theoretical metrics applied to a network with nodes (predefined ROIs) and edges (functional connections between ROIs) provide powerful tools to quantify such topographical alterations. Thus, the correlation matrices defined above were used to assess the graph theoretical metrics of mean characteristic path length, mean local efficiency, mean clustering coefficient, and mean betweenness centrality and small-worldness—indices that characterize network properties and the efficiency of information transfer. Calculated as the average length of the shortest path between two nodes, the mean characteristic path length denotes the level of integration in a given network and is inversely related to the global efficiency of information transfer. Mean local efficiency, on the other hand, measures global efficiency on the neighbourhood sub-graphs. Related to the clustering coefficient, which measures the likelihood of a given node's neighbours to be also connected to each other, these two measures allude to the level of integration/segregation in a network, and how efficient the communication is at the local level. Betweenness centrality is a measure of node degree

Table 1
Network specific ROIs selected for the functional connectivity analysis. The 14 somatomotor ROIs were chosen from the local peaks of the *task* > *fixation* contrast of the finger opposition paradigm. The 16 DMN ROIs on the other hand were chosen from the available literature. A 6 mm sphere was placed on all the 30 ROIs for further seed-based functional connectivity analyses.

Default mode ROIs			Somatomotor ROIs		
MNI [x y z]	Abbreviation	Nomenclature	MNI [x y z]	Abbreviation	Nomenclature
[0 52 26]	dMPFC	Dorsal medial prefrontal cortex	[−4 −2 54]	SMA	Supplementary motor area
[−6 52 −2]	aMPFC	Anterior medial prefrontal cortex	[−36 −22 64]	LPreCG	Left precentral gyrus
[0 26 −18]	vMPFC	Ventral medial prefrontal cortex	[60 8 28]	RPreCG	Right precentral gyrus
[−44 −74 32]	LpIPL	Left posterior inferior parietal lobe	[−40 −26 52]	LPoCG	Left postcentral gyrus
[44 −74 32]	RpIPL	Right posterior inferior parietal lobe	[56 −16 38]	RPoCG	Right postcentral gyrus
[−54 −54 28]	LTPJ	Left temporal parietal junction	[−14 −20 2]	LTHA	Left thalamus
[54 −54 28]	RTPJ	Right temporal parietal junction	[14 −20 2]	RTHA	Right thalamus
[−60 −24 −18]	LLTC	Left lateral temporal cortex	[−20 −8 −2]	LPAL	Left pallidum
[60 −24 −18]	RLTC	Right lateral temporal cortex	[20 −8 −2]	RPAL	Right pallidum
[0 −58 27]	PCC	Posterior cingulate cortex	[−22 −54 −24]	LCer6	Left cerebellar lobule 6
[−14 −52 8]	LRsp	Left retrosplenial cortex	[22 −58 −24]	RCer6	Right cerebellar lobule 6
[14 −52 8]	RRsp	Right retrosplenial cortex	[−14 −64 −46]	LCer8	Left cerebellar lobule 8
[−27 −15 26]	LPHC	Left parahippocampal cortex	[14 −64 −46]	RCer8	Right cerebellar lobule 8
[27 −15 26]	RPHC	Right parahippocampal cortex	[6 −62 20]	Ver6	Vermis lobule 6
[−28 −15 −12]	LHF+	Left hippocampal formation			
[28 −15 −12]	RHF+	Right hippocampal formation			

(number of connections) and indicates the relative importance of each node calculated as the ratio of shortest paths in the network that passes through a node (Rubinov and Sporns, 2010). Last but not least, small-worldness denotes a biologically relevant network topology with dense local clustering and limited long-range connections (Bassett et al., 2006). In addition, clustering coefficient, degree, local efficiency and betweenness centrality were measured at the node level and included in the supplementary information. The analysis of these metrics and the corresponding statistical differences across conditions were calculated using the Graph-Theoretical Analysis Toolbox (GAT) (Hosseini et al., 2012) based on the Brain Connectivity Toolbox (BCT) (Rubinov and Sporns, 2010). The initial step involved the selection of a range of threshold densities (T) at which the correlation matrices would be binarized. The goal was to establish a lower limit at which the nodes remained fully connected and an upper limit where the networks still displayed biologically plausible small-world architecture (Bassett et al., 2008). The range was measured as $0.2 < T < 0.4$. The same metrics were calculated for 20 random networks and compared to the original network over 5000 permutations (Tomson et al., 2013) using the area under the curve (AUC) method. The reported p-values were multiple comparisons corrected using FDR at the 0.05 level of significance.

Results

Contrast specific activity

With the aim of identifying study specific ROIs for the subsequent functional connectivity analysis and to confirm that the finger opposition paradigm activated a motor related network as expected, we focused the initial investigation on activity elicited by the task. The contrast of *task* > *fixation* produced a set of clusters associated with motor tasks (Kasahara et al., 2010) with a global peak in the left precentral gyrus and local peaks in the left pre and postcentral motor cortices, supplementary motor area, left thalamus, left pallidum, and bilateral cerebellum with a right hemispheric bias (Supplementary Fig. S1).

Topographical modulation of functional connectivity

The objective of the subsequent functional connectivity analysis was to compare and contrast the topography of the DMN and SMN during task and fixation conditions but also at rest with the aim of identifying potential task-induced network alterations. The ROI-to-voxel functional connectivity was estimated using the seed-based technique, and the corresponding network maps were carried forward on to group level statistical analyses. While the left precentral gyrus, identified from the subtractive analysis, served as the seed for SMN (MNI: 0 −58 27), a literature-based hub of the DMN on the posterior cingulate cortex (MNI: −36 −22 −64) was utilized as the network seed (Andrews-Hanna et al., 2010).

The posterior cingulate cortex functional connectivity revealed a DMN in all three conditions with important topological differences that are in line with previous studies of attention demanding tasks (Fransson, 2006). The F-contrast in a within subject one-way ANOVA across the three experimental conditions resulted in significant changes in left precuneus, bilateral angular gyri, right middle temporal cortex and left anterior cingulate cortex. The contrast estimates of the five statistical peaks revealed relatively higher connectivity at rest in comparison with the finger opposition paradigm (Fig. 1A). However, the task and fixation conditions did not show a significant difference from each other. In the case of the left precentral gyrus functional connectivity analysis for the SMN, the F-contrast revealed alterations that extended from right postcentral gyri to right cerebellar 4th and 6th lobules (Supplementary Fig. S2). Detailed post-hoc t-test results are available in the Supplementary Tables S1–2.

Behavioural correlation of functional networks

Given our hypothesis on the involvement of the DMN in cognitive processing, our next objective was to assess whether DMN (posterior cingulate cortex seed) connectivity across the three conditions related to a measure of motor processing. We used the CANTAB simple reaction time task as a proxy for performance (mean SRT = 0.24 s, SD = 0.03). The task requires the participants to press a button in response to a visual stimulus and provides a reliable measure of motor processing abilities (Gilbert et al., 2006). In both the task and fixation conditions greater connectivity of the DMN with a left superior frontal gyrus cluster predicted lower simple reaction time score, thus faster processing (Fig. 1B). While the superior frontal gyrus cluster in the task condition contained left superior frontal (MNI: −28 66 12), medial frontal (MNI: −12 58 10), and left middle frontal (MNI: −26 62 4) regions, the cluster in the fixation condition comprised a left middle frontal peak (MNI: −22 42 26). The results are in line with a previous study, in which an increased coupling between the posterior cingulate cortex and medial prefrontal cortex was associated with better performance (Hampson et al., 2006). Crucially, there was no significant correlation between behaviour and DMN connectivity at rest.

Reconfiguration of functional networks

The following step in our analysis was to examine the interaction between the DMN and SMN by exploring any potential alterations in their clustering during the finger opposition conditions of task and fixation in comparison with rest. In light of recent evidence suggesting DMN interaction with other large-scale brain networks during goal-driven paradigms (Spreng et al., 2013), our objective was to reveal the extent of DMN interaction with the task-related SMN during the finger opposition paradigm. At first, Pearson correlation coefficients were calculated for the data series obtained from 6 mm diameter spherical seeds placed on a total of 30 ROIs. While 16 DMN regions were selected from the literature (Andrews-Hanna et al., 2010), 14 SMN regions were based on the statistical peaks of the activation analysis. The MNI coordinates are listed in Table 1. The resulting correlation matrices (30×30 ROIs) for each experimental condition were hierarchically separated into two clusters based on their functional similarity, and the results were visualized using connectograms (Irimia et al., 2012).

At rest, the clustering algorithm could independently divide the 30 ROIs into the DMN (16 ROIs) and SMN (14 ROIs) (Fig. 2). However, during the finger opposition paradigm, there were important realignments in the clustering of the 30 ROIs. In the task condition, left cerebellum, left pallidum and bilateral thalamus switched memberships from SMN to DMN. Nevertheless, the left thalamus preserved significant connections with the left pre and post central gyri, which were in turn connected to the left hippocampal formation. The right pallidum on the other hand, did not show any significant connections in this network. During the fixation condition, the entire medial prefrontal cortex ROIs, bilateral lateral temporal cortices and bilateral lateral temporo-parietal junction areas moved from the DMN cluster to the SMN. Nonetheless, significant connections remained between the medial prefrontal cortex areas, posterior cingulate cortex and left posterior inferior parietal lobe (see Fig. 2). Moreover, bilateral thalamus had no significant network connections. Important characteristics to emphasize are the strong intra-network connections and the pronounced inter-network anti-correlations at rest in comparison with the two finger opposition conditions.

Graph theoretical readjustments of functional networks

The observed alterations in the network configuration of 30 ROI-to-ROI correlations were quantitatively assessed by comparing graph theoretical measures across the three different experimental conditions. In this context, small-worldness examines the biologically relevant reconfiguration of global brain connections under varying environmental

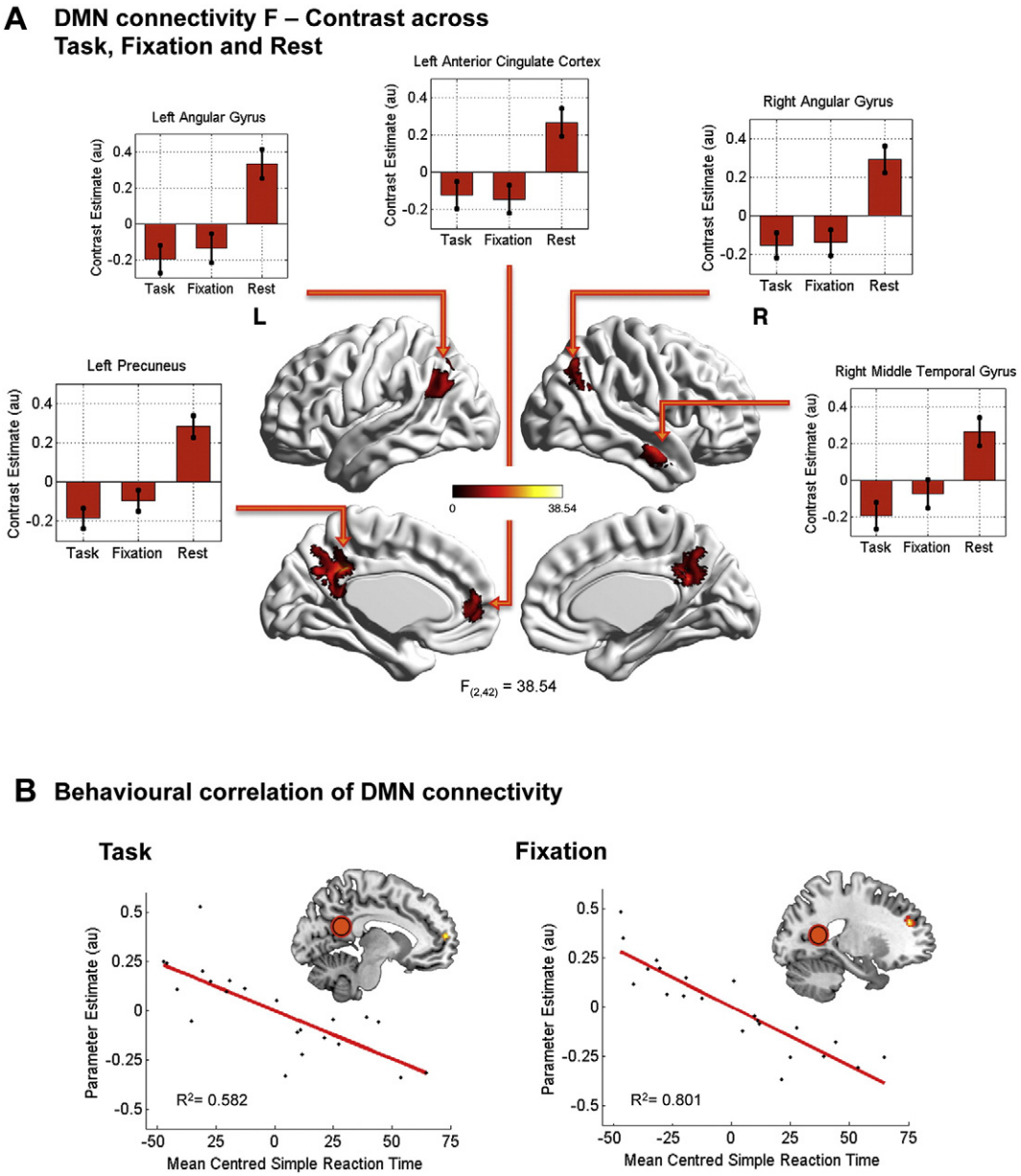

Fig. 1. DMN functional connectivity and behavioural correlation. (A) Topographical changes in the DMN functional connectivity based on an F-Contrast across task, fixation and rest conditions. The contrast estimates (arbitrary units—au) of the five reported clusters (cluster level FWE correction, $p < 0.05$) revealed greater connectivity at rest in comparison with task and fixation blocks of the finger opposition paradigm. (B) Behavioural correlation of DMN connectivity across the three experimental conditions. Greater connectivity between DMN (based on posterior cingulate cortex seed represented by the red sphere) and left superior frontal gyrus, including left superior frontal (MNI: −28 66 12), medial frontal (MNI: −12 58 10), left middle frontal (MNI: −26 62 4) gyri for the task condition, and left middle frontal gyrus (MNI: −22 42 26) for the fixation condition, predicted lower simple reaction time score, thus better performance. DMN connectivity at rest did not relate to the behavioural score.

conditions for an optimal architecture between the efficiency of information processing and cost of wiring (Achard et al., 2006). On the other hand, metrics such as mean characteristic path length, clustering coefficient, local efficiency and betweenness centrality refer to the global parallel processing power and efficacy in information transfer (Rubinov and Sporns, 2010). While mean characteristic path length, clustering coefficient and local efficiency denote the level of integration and segregation in a given network for optimal information transfer, betweenness centrality alludes to the relative importance of network nodes.

Although no global network metric comparison between the task and fixation periods survived correction for multiple comparisons ($P_{FDR} < 0.05$), the two conditions showed significant differences in their network properties when contrasted against the resting state scan. In comparison with rest, the motor task showed shorter mean characteristic path length ($P_{FDR} = 0.0080$), smaller mean clustering coefficient ($P_{FDR} = 0.0030$), smaller mean local efficiency ($P_{FDR} = 0.010$) and smaller mean betweenness centrality ($P_{FDR} = 0.0093$) and no difference in the small-worldness measure ($P_{FDR} = 0.59$). The fixation condition in comparison with rest on the other hand, revealed shorter mean characteristic path length ($P_{FDR} = 0.029$), smaller mean clustering coefficient ($P_{FDR} = 0.0040$) and smaller mean local efficiency ($P_{FDR} = 0.027$), and no difference in either the mean betweenness centrality ($P_{FDR} = 0.057$) or the mean small-worldness measure ($P_{FDR} = 0.30$). Previous studies on the network level brain architecture have also revealed persistence in the small-world properties of the brain organization across motor skill acquisition (Bassett et al., 2006, 2011). Focusing on the node characteristics, the DMN regions illustrated the greatest

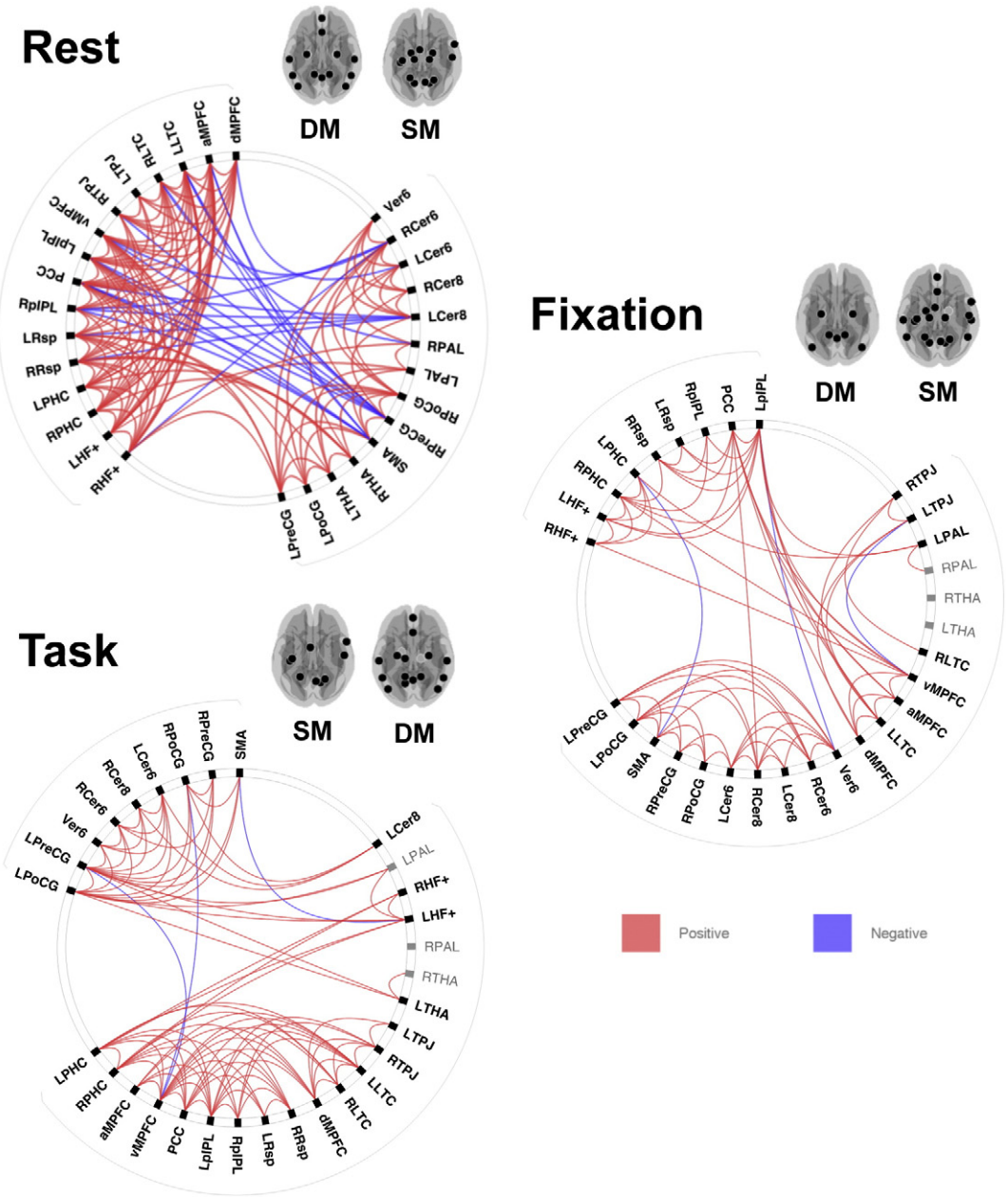

Fig. 2. Hierarchically clustered ROI-to-ROI connectivity of the default mode and somatomotor regions across three experimental conditions. Pearson correlation coefficient matrices of 30 ROIs were hierarchically clustered into the default mode (DM) and somatomotor (SM) domains according to their functional similarity. Red and blue lines represent positive and negative correlations, respectively. The MNI positions of the selected ROIs are symbolized in the transparent axial brain clusters around the ring. The reported clusters are corrected for multiple comparisons using the network based statistics permutation testing at the 0.05 level of significance and the grayed out labels represent the ROIs that did not reach significance in their network connections. The abbreviations and the associated nomenclature are given in Table 1.

overall importance in terms of magnitude across all metrics and all three experimental conditions. Notably, the posterior cingulate cortex illustrated the highest degree across the three experimental conditions. The complete results are summarized in Supplementary Table S3.

Discussion

The specific aims of our study were i) to identify topological changes in functional connectivity of the DMN across the three distinct experimental conditions, ii) to relate DMN connectivity to behaviour, iii) to evaluate whether any DMN regions would change network affiliation in response to task demands, and iv) to quantify the alterations in network reconfiguration via graph theoretical analysis. Overall, our results demonstrate a DMN that does not disintegrate during task execution but instead changes topology and configuration, suggesting a possible DMN involvement in task performance.

Modulation of default mode functional connectivity

Since the discovery of the spatially structured, intrinsic oscillations of the motor brain areas (Biswal et al., 1995), the cognitive neuroscience literature has witnessed a surge in the amount of task-free and task-based functional connectivity analyses aiming to investigate the large-scale human brain network organization and to explain their relevance to cognition. Studies comparing task to rest across different cognitive domains report variability in the direction of connectivity changes for

individual large-scale brain networks, but also an overall decrease in global functional network connectivity in the task condition (Arbabshirani et al., 2013; Bartels and Zeki, 2005).

Our analyses revealed a robustly connected DMN across all three conditions, largely in agreement with previous studies investigating large-scale network changes when comparing task to rest (Arbabshirani et al., 2013; Calhoun et al., 2008). Greater DMN connectivity was observed at rest as opposed to the task and fixation conditions of the finger opposition paradigm. Although the functional connectivity of the DMN in an active motor task has not been previously studied, similar research using a variety of other cognitive paradigms, has suggested persistent DMN functional connectivity during task execution (Arbabshirani et al., 2013; Fransson and Marrelec, 2008). One such example is a passive listening paradigm, which revealed persisting DMN connectivity during both the fixation and task blocks (Hasson et al., 2009). Importantly, DMN topography changes were observed when comparing the two conditions. Altogether, these findings propose a wider role for the DMN than previously ascribed to this network.

At the cluster level, the comparison across the three experimental conditions revealed significant changes in the functional connectivity of the DMN at the left precuneus, bilateral angular gyri, right middle temporal cortex and left anterior cingulate cortex. A growing number of studies differentiate the functionality of the precuneus from its anatomical neighbour, the posterior cingulate cortex, on the basis of its potential role in mediating connections between the default mode and the fronto-parietal control networks (Leech et al., 2011; Margulies et al., 2009; Spreng et al., 2013). Together these two networks may fulfil the demands required by the task at hand. From a cognitive standpoint, bilateral angular gyri have been implicated in the temporary storage of information, whereas the left anterior cingulate cortex has been associated with conflict monitoring in goal-driven tasks (Vincent et al., 2008), processes that might have been attenuated by our motor task. Taken together, the results allude to a change in the interaction of the DMN with the fronto-parietal control network and point to involvement in the finger opposition task execution.

Furthermore, our results illustrated that DMN connectivity with the left superior frontal gyrus (extending to medial frontal and left middle frontal gyri) both during task and fixation conditions predicted motor performance measured outside the scanner. There is evidence showing that medial superior frontal areas are involved in motor planning (Spreng et al., 2013) (relevant to the task employed in this experiment) and increased activation in the medial prefrontal cortex during a simple reaction time task was shown to correlate with performance reflecting the contribution of DMN to motor task execution (Gilbert et al., 2006). Moreover, the superior frontal gyri are arguably part of the DMN and recent research suggests that they may mediate the network's connection to the fronto-parietal control network in order to facilitate goal-directed behaviour (Spreng et al., 2010) and are associated with working memory tasks (du Boisgueheneuc et al., 2006). Remarkably, although a substantial volume of earlier work suggests that DMN activity during task might be related to task-irrelevant, stimulus independent thoughts (McKiernan et al., 2006), our results indicate that DMN connectivity during task and fixation conditions (but not at rest) was associated with faster reaction time in the finger opposition task.

In summary, the outcome of this study not only signifies that the traditional activation contrasts do not provide a full account of the underlying neural processes, thereby making a case for the wider use of task-based functional connectivity, but further suggests that the fixation periods in a given paradigm cannot be considered as true rest and that they are affected by the employed task blocks. Future research will require the addition of fronto-parietal control and dorsal attention networks with a greater number of ROIs for a wider picture of the underlying network interactions and reconfigurations during motor task execution. The outcome of such studies would bring us closer to deciphering the exact mechanism of action of the DMN.

Interaction of default mode and somatomotor regions

The observed network topographical differences between the three experimental conditions of interest in our ROI-to-ROI analysis indicate that certain brain regions dynamically change their network membership during task performance and interact with other large-scale networks to possibly fulfil task requirements. In the case of DMN and SMN, we observed the realignment of the left cerebellum, left pallidum and bilateral thalamus to the default mode domain at task condition. A growing number of studies focus on the contribution of the cerebellum to higher cognitive functions (Stoodley, 2012) and highlight its functional connectivity with the neocortex (Habas et al., 2009). The membership switch we observed in the cerebellar and deep grey matter structures might represent associative learning and motivational assignments to the ongoing motor task demands (Pasupathy and Miller, 2005). Moreover, during the fixation period, all the medial prefrontal cortex ROIs, bilateral lateral temporal cortices and bilateral lateral temporo-parietal junction areas changed their alignment from DMN to SMN. All of these regions have been implicated in mediating the connection of the DMN to other large-scale networks, e.g. fronto-parietal control network, which may suggest task-induced changes in the interaction of default mode and somatomotor regions.

Other noteworthy differences between task, fixation and rest, investigated in this study are the anti-correlations between the default mode and somatomotor regions in the task and fixation periods as compared to the resting state scan. Although there is an ongoing debate about the influence of analysis techniques on the introduction of the detected anti-correlations in BOLD signal (Murphy et al., 2009), growing evidence emphasizes the biological relevance of these observations in consideration with the potential contribution of methodological confounds (Chai et al., 2012; Fox et al., 2009). Given that all the data used in this study was pre-processed and analysed in exactly the same manner, we may infer that the observed anti-correlations have a neural basis that remains to be elucidated.

Efficient and preserved global network architecture

The graph theoretical analysis provides quantitative support for network level changes induced by the finger opposition paradigm in comparison with the resting state scan. Bassett and colleagues suggest that the global topology (small-world architecture) is preserved during task performance, but with an increase in long-range brain connections (Bassett et al., 2006). Our observations concur with this conclusion since we found no differences in small-worldness between the three experimental conditions. Large-scale brain networks were previously shown to present biologically relevant small-world architecture which reflects the underlying structural connectivity (Achard et al., 2006). However, when compared to rest, both the task and fixation conditions showed shorter mean characteristic path length, smaller mean clustering coefficient and less local efficiency. A shorter mean characteristic path length has been associated with high global efficiency of parallel information transfer, denoting fewer edges that need to be transversed in order to reach one node from another, and thus longer range connections that form between the nodes of the network (Wang et al., 2010). Furthermore, a smaller clustering coefficient indicates a less cliquey, thus more random, network structure (Bullmore and Sporns, 2012); an observation that is also supported by the decrease in local efficiency. Finally, the node analysis largely indicated the DMN region as showing the highest metrics across the three experimental conditions, placing great importance on the posterior cingulate cortex as the ROI with the highest degree, denoting the number of connections made.

In brief, the two networks show transient changes in the interactions between their constituent parts but overall preserved global brain architecture. Our results comply with the theoretical accounts proposing that transient environmental demands produce task-induced changes in brain organization (Kitzbichler et al., 2011); however, global-brain

network properties remain constant. Taken together with our functional connectivity results, the graph theoretical analysis also places a special importance on the DMN as a connector hub across all three conditions, and indicates its interaction with somatomotor regions to fulfil task requirements.

Conclusion

The last decade has seen a surge in the number of neuroimaging studies that revealed the intrinsic neural synchrony of distant brain regions. Despite the advancements made in their topographical characterization at rest, the behavioural significance of large-scale brain networks especially that of DMN, remains to be elucidated. In this context, our results provide important information on the changing relationship between the DMN and SMN as we observed volunteers at rest, fixation and finger-opposition task conditions. Our findings suggest persistence of DMN connectivity during task execution, thus providing evidence that has not been previously described, and alluding to a DMN function that surpasses the accounts of spontaneous internal mentation. Nevertheless, more task and rest based research with comprehensive analytical techniques and cognitive paradigms will be required to decipher the exact contribution of the DMN to human cognition.

Acknowledgments

The Evelyn Trust (RUAG/018) provided the required funding for this research. Additionally, D Vatansever is funded by the Yousef Jameel Academic Program administered via the Cambridge Commonwealth, European and International Trust; DK Menon is supported by funding from the NIHR Cambridge Biomedical Centre (RCZB/004), and an NIHR Senior Investigator Award (RCZB/014), and EA Stamatakis is funded by the Stephen Erskine Fellowship Queens' College Cambridge. We would also like to thank Sanja Abbott for programming the stimulus delivery, Dr. Guy Williams and Victoria Lupson and the rest of the staff in the Wolfson Brain Imaging Centre (WBIC) at Addenbrooke's Hospital for their assistance in scanning. Last but not least, we thank all the participants for their contribution to this study.

Appendix A. Supplementary data

Supplementary data to this article can be found online at http://dx.doi.org/10.1016/j.neuroimage.2015.07.053.

References

Achard, S., Salvador, R., Whitcher, B., Suckling, J., Bullmore, E., 2006. A resilient, low-frequency, small-world human brain functional network with highly connected association cortical hubs. J. Neurosci. 26, 63–72.
Andrews-Hanna, J.R., Reidler, J.S., Huang, C., Buckner, R.L., 2010. Evidence for the default network's role in spontaneous cognition. J. Neurophysiol. 104, 322–335.
Arbabshirani, M.R., Havlicek, M., Kiehl, K.A., Pearlson, G.D., Calhoun, V.D., 2013. Functional network connectivity during rest and task conditions: a comparative study. Hum. Brain Mapp. 34, 2959–2971.
Bartels, A., Zeki, S., 2005. Brain dynamics during natural viewing conditions: a new guide for mapping connectivity in vivo. NeuroImage 24, 339–349.
Bassett, D.S., Meyer-Lindenberg, A., Achard, S., Duke, T., Bullmore, E., 2006. Adaptive reconfiguration of fractal small-world human brain functional networks. Proc. Natl. Acad. Sci. U. S. A. 103, 19518–19523.
Bassett, D.S., Bullmore, E., Verchinski, B.A., Mattay, V.S., Weinberger, D.R., Meyer-Lindenberg, A., 2008. Hierarchical organization of human cortical networks in health and schizophrenia. J. Neurosci. 28, 9239–9248.
Bassett, D.S., Wymbs, N.F., Porter, M.A., Mucha, P.J., Carlson, J.M., Grafton, S.T., 2011. Dynamic reconfiguration of human brain networks during learning. Proc. Natl. Acad. Sci. U. S. A. 108, 7641–7646.
Behzadi, Y., Restom, K., Liau, J., Liu, T.T., 2007. A component based noise correction method (CompCor) for BOLD and perfusion based fMRI. NeuroImage 37, 90–101.
Binder, J.R., Frost, J.A., Hammeke, T.A., Bellgowan, P.S., Rao, S.M., Cox, R.W., 1999. Conceptual processing during the conscious resting state. A functional MRI study. J. Cogn. Neurosci. 11, 80–95.
Biswal, B., Yetkin, F.Z., Haughton, V.M., Hyde, J.S., 1995. Functional connectivity in the motor cortex of resting human brain using echo-planar MRI. Magn. Reson. Med. 34, 537–541.
Buckner, R.L., Sepulcre, J., Talukdar, T., Krienen, F.M., Liu, H., Hedden, T., Andrews-Hanna, J.R., Sperling, R.A., Johnson, K.A., 2009. Cortical hubs revealed by intrinsic functional connectivity: mapping, assessment of stability, and relation to Alzheimer's disease. J. Neurosci. 29, 1860–1873.
Bullmore, E., Sporns, O., 2012. The economy of brain network organization. Nat. Rev. Neurosci. 13, 336–349.
Calhoun, V.D., Kiehl, K.A., Pearlson, G.D., 2008. Modulation of temporally coherent brain networks estimated using ICA at rest and during cognitive tasks. Hum. Brain Mapp. 29, 828–838.
Chai, X.J., Castañón, A.N., Ongür, D., Whitfield-Gabrieli, S., 2012. Anticorrelations in resting state networks without global signal regression. NeuroImage 59, 1420–1428.
Damoiseaux, J.S., Beckmann, C.F., Arigita, E.J.S., Barkhof, F., Scheltens, P.H., Stam, C.J., Smith, S.M., Rombouts, S.A.R.B., 2008. Reduced resting-state brain activity in the "default network" in normal aging. Cereb. Cortex 18, 1856–1864.
Dosenbach, N.U.F., Fair, D.A., Miezin, F.M., Cohen, A.L., Wenger, K.K., Dosenbach, R.A.T., Fox, M.D., Snyder, A.Z., Vincent, J.L., Raichle, M.E., Schlaggar, B.L., Petersen, S.E., 2007. Distinct brain networks for adaptive and stable task control in humans. Proc. Natl. Acad. Sci. U. S. A. 104, 11073–11078.
du Boisgueheneuc, F., Levy, R., Volle, E., Seassau, M., Duffau, H., Kinkingnehun, S., Samson, Y., Zhang, S., Dubois, B., 2006. Functions of the left superior frontal gyrus in humans: a lesion study. Brain 129, 3315–3328.
Fair, D.A., Schlaggar, B.L., Cohen, A.L., Miezin, F.M., Dosenbach, N.U.F., Wenger, K.K., Fox, M.D., Snyder, A.Z., Raichle, M.E., Petersen, S.E., 2007. A method for using blocked and event-related fMRI data to study "resting state" functional connectivity. NeuroImage 35, 396–405.
Fox, M.D., Snyder, A.Z., Vincent, J.L., Corbetta, M., Van Essen, D.C., Raichle, M.E., 2005. The human brain is intrinsically organized into dynamic, anticorrelated functional networks. Proc. Natl. Acad. Sci. U. S. A. 102, 9673–9678.
Fox, M.D., Zhang, D., Snyder, A.Z., Raichle, M.E., 2009. The global signal and observed anticorrelated resting state brain networks. J. Neurophysiol. 101, 3270–3283.
Fransson, P., 2006. How default is the default mode of brain function? Further evidence from intrinsic BOLD signal fluctuations. Neuropsychologia 44, 2836–2845.
Fransson, P., Marrelec, G., 2008. The precuneus/posterior cingulate cortex plays a pivotal role in the default mode network: evidence from a partial correlation network analysis. NeuroImage 42, 1178–1184.
Gilbert, S.J., Simons, J.S., Frith, C.D., Burgess, P.W., 2006. Performance-related activity in medial rostral prefrontal cortex (area 10) during low-demand tasks. J. Exp. Psychol. 32, 45–58.
Greicius, M.D., Krasnow, B., Reiss, A.L., Menon, V., 2003. Functional connectivity in the resting brain: a network analysis of the default mode hypothesis. Proc. Natl. Acad. Sci. U. S. A. 100, 253–258.
Greicius, M.D., Supekar, K., Menon, V., Dougherty, R.F., 2009. Resting-state functional connectivity reflects structural connectivity in the default mode network. Cereb. Cortex 19, 72–78.
Gusnard, D.A., Raichle, M.E., 2001. Searching for a baseline: functional imaging and the resting human brain. Nat. Rev. Neurosci. 2, 685–694.
Gusnard, D.A., Akbudak, E., Shulman, G.L., Raichle, M.E., 2001. Medial prefrontal cortex and self-referential mental activity: relation to a default mode of brain function. Proc. Natl. Acad. Sci. U. S. A. 98, 4259–4264.
Habas, C., Kamdar, N., Nguyen, D., Prater, K., Beckmann, C.F., Menon, V., Greicius, M.D., 2009. Distinct cerebellar contributions to intrinsic connectivity networks. J. Neurosci. 29, 8586–8594.
Hagmann, P., Cammoun, L., Gigandet, X., Meuli, R., Honey, C.J., Wedeen, V.J., Sporns, O., 2008. Mapping the structural core of human cerebral cortex. PLoS Biol. 6, e159.
Hampson, M., Driesen, N.R., Skudlarski, P., Gore, J.C., Constable, R.T., 2006. Brain connectivity related to working memory performance. J. Neurosci. 26, 13338–13343.
Harrison, B.J., Pujol, J., López-Solà, M., Hernández-Ribas, R., Deus, J., Ortiz, H., Soriano-Mas, C., Yücel, M., Pantelis, C., Cardoner, N., 2008. Consistency and functional specialization in the default mode brain network. Proc. Natl. Acad. Sci. U. S. A. 105, 9781–9786.
Hasson, U., Nusbaum, H.C., Small, S.L., 2009. Task-dependent organization of brain regions active during rest. Proc. Natl. Acad. Sci. U. S. A. 106, 10841–10846.
Hosseini, S.M.H., Hoeft, F., Kesler, S.R., 2012. GAT: a graph-theoretical analysis toolbox for analyzing between-group differences in large-scale structural and functional brain networks. PLoS One 7, e40709.
Irimia, A., Chambers, M.C., Torgerson, C.M., Van Horn, J.D., 2012. Circular representation of human cortical networks for subject and population-level connectomic visualization. NeuroImage 60, 1340–1351.
Kasahara, M., Menon, D.K., Salmond, C.H., Outtrim, J.G., Taylor Tavares, J.V., Carpenter, T.A., Pickard, J.D., Sahakian, B.J., Stamatakis, E.A., 2010. Altered functional connectivity in the motor network after traumatic brain injury. Neurology 75, 168–176.
Kitzbichler, M.G., Henson, R.N., Smith, M.L., Nathan, P.J., Bullmore, E.T., 2011. Cognitive effort drives workspace configuration of human brain functional networks. J. Neurosci. 31, 8259–8270.
Laird, A.R., Fox, P.M., Eickhoff, S.B., Turner, J.A., Ray, K.L., McKay, D.R., Glahn, D.C., Beckmann, C.F., Smith, S.M., Fox, P.T., 2011. Behavioral interpretations of intrinsic connectivity networks. J. Cogn. Neurosci. 23, 4022–4037.
Leech, R., Kamourieh, S., Beckmann, C.F., Sharp, D.J., 2011. Fractionating the default mode network: distinct contributions of the ventral and dorsal posterior cingulate cortex to cognitive control. J. Neurosci. 31, 3217–3224.
Margulies, D.S., Vincent, J.L., Kelly, C., Lohmann, G., Uddin, L.Q., Biswal, B.B., Villringer, A., Castellanos, F.X., Milham, M.P., Petrides, M., 2009. Precuneus shares intrinsic functional architecture in humans and monkeys. Proc. Natl. Acad. Sci. U. S. A. 106, 20069–20074.

Mazoyer, B., Zago, L., Mellet, E., Bricogne, S., Etard, O., Houdé, O., Crivello, F., Joliot, M., Petit, L., Tzourio-Mazoyer, N., 2001. Cortical networks for working memory and executive functions sustain the conscious resting state in man. Brain Res. Bull. 54, 287–298.

McKiernan, K.A., D'Angelo, B.R., Kaufman, J.N., Binder, J.R., 2006. Interrupting the "stream of consciousness": an fMRI investigation. NeuroImage 29, 1185–1191.

Murphy, K., Birn, R.M., Handwerker, D.A., Jones, T.B., Bandettini, P.A., 2009. The impact of global signal regression on resting state correlations: are anti-correlated networks introduced? NeuroImage 44, 893–905.

Newton, A.T., Morgan, V.L., Rogers, B.P., Gore, J.C., 2011. Modulation of steady state functional connectivity in the default mode and working memory networks by cognitive load. Hum. Brain Mapp. 32, 1649–1659.

Pasupathy, A., Miller, E.K., 2005. Different time courses of learning-related activity in the prefrontal cortex and striatum. Nature 433, 873–876.

Power, J.D., Cohen, A.L., Nelson, S.M., Wig, G.S., Barnes, K.A., Church, J.A., Vogel, A.C., Laumann, T.O., Miezin, F.M., Schlaggar, B.L., Petersen, S.E., 2011. Functional network organization of the human brain. Neuron 72, 665–678.

Raichle, M.E., MacLeod, A.M., Snyder, A.Z., Powers, W.J., Gusnard, D.A., Shulman, G.L., 2001. A default mode of brain function. Proc. Natl. Acad. Sci. U. S. A. 98, 676–682.

Rubinov, M., Sporns, O., 2010. Complex network measures of brain connectivity: uses and interpretations. NeuroImage 52, 1059–1069.

Schacter, D.L., Addis, D.R., Hassabis, D., Martin, V.C., Spreng, R.N., Szpunar, K.K., 2012. The future of memory: remembering, imagining, and the brain. Neuron 76, 677–694.

Sharp, D.J., Beckmann, C.F., Greenwood, R., Kinnunen, K.M., Bonnelle, V., De Boissezon, X., Powell, J.H., Counsell, S.J., Patel, M.C., Leech, R., 2011. Default mode network functional and structural connectivity after traumatic brain injury. Brain 134, 2233–2247.

Shulman, G.L., Fiez, J.A., Corbetta, M., Buckner, R.L., Miezin, F.M., Raichle, M.E., Petersen, S.E., 1997. Common blood flow changes across visual tasks: II. Decreases in cerebral cortex. J. Cogn. Neurosci. 9, 648–663.

Smith, S.M., Fox, P.T., Miller, K.L., Glahn, D.C., Fox, P.M., Mackay, C.E., Filippini, N., Watkins, K.E., Toro, R., Laird, A.R., Beckmann, C.F., 2009. Correspondence of the brain's functional architecture during activation and rest. Proc. Natl. Acad. Sci. U. S. A. 106, 13040–13045.

Smith, S.M., Miller, K.L., Salimi-Khorshidi, G., Webster, M., Beckmann, C.F., Nichols, T.E., Ramsey, J.D., Woolrich, M.W., 2011. Network modelling methods for FMRI. NeuroImage 54, 875–891.

Spreng, R.N., Stevens, W.D., Chamberlain, J.P., Gilmore, A.W., Schacter, D.L., 2010. Default network activity, coupled with the frontoparietal control network, supports goal-directed cognition. NeuroImage 53, 303–317.

Spreng, R.N., Sepulcre, J., Turner, G.R., Stevens, W.D., Schacter, D.L., 2013. Intrinsic architecture underlying the relations among the default, dorsal attention, and frontoparietal control networks of the human brain. J. Cogn. Neurosci. 25, 74–86.

Stamatakis, E.A., Adapa, R.M., Absalom, A.R., Menon, D.K., 2010. Changes in resting neural connectivity during propofol sedation. PLoS One 5, e14224.

Stoodley, C.J., 2012. The cerebellum and cognition: evidence from functional imaging studies. Cerebellum 11, 352–365.

Tomson, S.N., Narayan, M., Allen, G.I., Eagleman, D.M., 2013. Neural networks of colored sequence synesthesia. J. Neurosci. 33, 14098–14106.

van den Heuvel, M.P., Sporns, O., 2011. Rich-club organization of the human connectome. J. Neurosci. 31, 15775–15786.

Vincent, J.L., Kahn, I., Snyder, A.Z., Raichle, M.E., Buckner, R.L., 2008. Evidence for a frontoparietal control system revealed by intrinsic functional connectivity. J. Neurophysiol. 100, 3328–3342.

Wang, J., Zuo, X., He, Y., 2010. Graph-based network analysis of resting-state functional MRI. Front. Syst. Neurosci. 4, 16.

Whitfield-Gabrieli, S., Nieto-Castanon, A., 2012. Conn: a functional connectivity toolbox for correlated and anticorrelated brain networks. Brain Connect. 2, 125–141.

Zalesky, A., Fornito, A., Bullmore, E.T., 2010. Network-based statistic: identifying differences in brain networks. NeuroImage 53, 1197–1207.